TSUNAMI-MAGNETIC SIGNALS AND MAGNETIC ANOMALY GENERATED BY TSUNAMI WAVE PROPAGATION AT OPEN SEAS

T. Prastowo[1, 2*], L. Cholifah[1], L. O. Ngkoimani[3], L. O. Safiuddin[3]

[1]Jurusan Fisika, FMIPA, Universitas Negeri Surabaya, Indonesia
[2]Pusat Studi Ilmu Bumi, FMIPA, Universitas Negeri Surabaya, Indonesia
[3]Jurusan Fisika, FMIPA, Universitas Halu Oleo, Kendari, Indonesia

ABSTRACT

This research examines the generation of tsunami-induced magnetic signals, where local magnetic anomaly were measured as variations in the vertical b_z and horizontal b_H components of the secondary field. The maximum amplitudes of b_z and b_H were analytically estimated and compared to magnetogram provided by INTERMAGNET and BCMT for the 2010 Chilean, the 2011 Tohoku, the 2010 Mentawai and the 2004 Aceh tsunamis. For the first two cases, frozen-flux theory was used to estimate b_z and b_H where the phase lag between b_z and b_H was $\pi/2$, relevant to time interval of $T/4$ between the two signals. For the Mentawai case, oceanic diffusion was unignored and b_z significantly deviated from that calculated using the theory. However, the data from Mentawai where $b_z \leq 2$ nT were in good agreement with b_z generated by large tsunamis occurring in regions near the equator and with magnetogram from the Aceh event.

ABSTRAK

Penelitian ini mempelajari pembangkitan sinyal magnetik akibat perambatan tsunami. Gangguan fisis pada permukaan laut menyebabkan anomali magnetik yang terukur sebagai variasi komponen vertikal b_z dan horisontal b_H medan sekunder. Amplitudo maksimum b_z dan b_H dihitung secara analitik dan dibandingkan dengan magnetogram dari INTERMAGNET dan BCMT untuk tsunami Chili 2010, Tohoku 2011, Mentawai 2010 dan Aceh 2004. Untuk kasus Chili 2010 dan Tohoku 2011, pendekatan *frozen-flux* secara efektif digunakan untuk estimasi b_z dan b_H di mana beda fase antara b_z dan b_H diprediksi $\pi/2$ yang setara dengan selang waktu $T/4$ antara kedua sinyal magnetik tersebut. Untuk kasus Mentawai 2010, difusi air laut tidak bisa diabaikan sehingga pendekatan *frozen-flux* menyimpang signifikan. Namun demikian, data kasus Mentawai 2010 di mana diperoleh $b_z \leq 2$ nT sesuai dengan estimasi analitik amplitudo maksimum b_z yang dibangkitkan oleh tsunami besar di wilayah ekuator yang ternyata juga sesuai dengan data magnetogram kasus Aceh 2004.

INTRODUCTION

This study examines tsunami-generated magnetic signals in the context of ocean dynamo effects, where the movement of electrically conducting seawater across the ambient geomagnetic field induces secondary magnetic fields (Tyler, 2005). Such perturbations on the sea surface produce local anomaly with respect to the Earth's magnetic field, which is measured as the vertical and horizontal components of the secondary field. Although the maximum amplitude of the local anomaly is relatively small compared to the main field, it can still be detected by sensitive instrument (Manoj, Maus, & Chulliat, 2011; Ichihara, Hamano, Baba, & Kasaya, 2013; Minami & Toh, 2013; Sugioka *et al*., 2014). The maximum amplitude is possibly determined by either analytical estimate or visual inspection upon magnetogram obtained from a global magnetic network of International

***Correspondence Address:**
Kampus Unesa Ketintang, Surabaya 60231
E-mail: prastowo.tjipto@gmail.com

Real-time Magnetic Observatory Network (INTERMAGNET) as reported by Klausner, Domingues, Mendes, & Papa (2011) and Bureau Central de Magnetisme Terrestre (BCMT) as used by Wang & Liu (2013). Similarities found in the vertical and horizontal components of the tsunami-magnetic signals between analytical estimate and visual inspection on magnetogram provided by the two global institutions are tested for several cases of large tsunamis.

Recent studies (*e.g.*, Tatehata, Ichihara, & Hamano, 2015) relevant to the generation of magnetic signals and local magnetic anomaly due to tsunami wave propagation have utilized numerical simulation to better understand mechanisms of production and variation of the secondary field. Other studies (*e.g.* Minami, Toh, & Tyler, 2015) have also been based on computational work examining effects of sea-depth parameter on tsunami wave propagation characteristic at open seas and determine whether advection or diffusion is the dominant physical process in a particular area in the ocean. As evaluated by Klausner, Kherani, & Muella (2016), a combined work of both computational techniques and field observations for determining the vertical component b_z of tsunami-induced signals revealed the same results obtained for separate considerations of near- and far-field distances from a tsunami source.

Minami *et al.* (2015) discussed the roles of ocean depth h in terms of a functional relationship between the external parameter (ocean diffusivity κ) and internal parameters (tsunami phase speed c and the complex speed of ocean waves c_s). By adopting ideas of Tyler (2005) and using research findings of Minami *et al.* (2015), we examine the dependence of local magnetic disturbance b_z/F_z where F_z denotes the vertical component of the main, Earth's magnetic field upon two dimensionless physical parameters, namely: h/L where $L = 2.53$ km is the characteristic lengthscale (Minami *et al.*, 2015) and c/c_s where c_s is defined as $c_s = c + ic_d$ with c_d is the rate of oceanic diffusion process (Tyler, 2001).

In this study, four large tsunami occurrences caused by earthquakes with magnitudes of $M_W \geq 7.8$ are separately examined and discussed, namely: the 2010 Chilean and the 2011 Tohoku events, where advection dominates over diffusion, and the 2010 Mentawai and the 2004 Aceh tsunamis, where oceanic diffusion cannot be ignored. Discussion for all cases focuses on the roles of important parameters h/L and c/c_s for use in determining a proper

formula to accurately estimate the vertical and horizontal signals of the tsunami-induced field.

As reported by Satriano, Wu, Zollo, & Kanamori (2011) and Satake (2014) in terms of concepts and methods of earth-related disaster risk reduction (for example, earthquakes and tsunamis), monitoring of tsunami-generated magnetic signals and the corresponding magnetic anomaly in the present study could thus be an alternative method for the development of a tsunami early warning system. Therefore, this research is expected to give shed light on researchers working on a similar subject and may then complete the existing method of seismic monitoring for tsunami early warning, such as the Indonesian Tsunami Early Warning System (Ina-TEWS) organized by the Indonesian Agency for Geophysics, Climatology, and Meteorology (BMKG). In addition, mechanisms of the generation of tsunami-magnetic signals and magnetic anomaly would be useful for enriched physics teaching materials in schools and universities. This is made possible because basic physic principles of such a phenomenon are derived from a set of Maxwell's equations, including the concept of electromagnetic induction widely known as Faraday and Biot-Savart laws, and Ohm's law for a moving conductor across magnetic lines of force.

METHOD

The governing equation required for examining fundamental mechanisms of the generation of tsunami-magnetic signals and magnetic anomaly in the oceans is as follows,

$$\partial_t b_z = -\nabla_H \cdot (F_z \mathbf{u}_H) + \kappa \nabla^2 b_z \qquad (1)$$

which is commonly known as the electromagnetic induction equation (Tyler, 2005; Ichihara *et al.*, 2013; Sugioka *et al.*, 2014; Minami *et al.*, 2015). The left-hand side of equation (1) describes time evolution of the vertical component b_z of the secondary field. The first term of the right-hand side denotes secondary field production by fluid flow of electrically conducting seawater (horizontal advection) while the second term represents contra-production of the secondary field by ocean local circulation (vertical diffusion).

Tyler (2005) evaluated the relative importance of each term on the right-hand side in equation (1) and reported that the ratio of local magnetic disturbance relative to the main geomagnetic field b_z/F_z is proportional to the ratio of local perturbation in the sea surface elevation relative to the ocean depth η/h. In this con-

text, η is the maximum vertical displacement of the sea surface owing to tsunami propagation. This idea was adopted and then further developed by Ichihara *et al.* (2013), Sugioka *et al.* (2014) and Minami *et al.* (2015) to derive equations necessary for estimating both the vertical b_z and horizontal b_H components of the tsunami-induced field. When oceanic diffusion can be neglected or in other words, horizontal advection dominates over vertical diffusion ($c/c_s \approx 1$), it is true that

$$b_z/F_z = \eta/h \qquad (2)$$

which is well known as *frozen-flux* approximation, commonly used for analytical estimate of b_z given that the other three variables in equation (2) are known. The horizontal component b_H of the induced field is then calculated from

$$b_H = i\, b_z \qquad (3)$$

which clearly indicates a phase difference between vertical and horizontal tsunami-magnetic signals.

Minami *et al.* (2015) found diffusion effects unignorable, particularly in parts of the ocean where $h/L < 2.0$ such that equation (2) becomes

$$b_z/F_z = c/c_s \times \eta/h \qquad (4)$$

The rate c_d of diffusion process at seas is defined as $c_d = 2\kappa/h$ and the phase speed c of a tsunami wave is written as $c = (gh)^{1/2}$ where g is the gravitational acceleration.

Equation (4) shows that the ratio of b_z/F_z depends upon the ocean depth h and is implicitly determined by two physical processes in the oceans, namely advection process represented by c and diffusion process denoted by c_d in terms of c/c_s. This parameter plays a role in determining which process is dominant over the other in the oceans. When $c/c_s \approx 1$ is satisfied, *frozen-flux* approximation holds and when $c/c_s < 1$, *frozen-flux* approximation gives estimate of b_z that significantly deviates from the expected value.

In line with zonal divisions at which a particular process is dominant in the oceans, Minami *et al.* (2015) proposed that oceanic zones are divided into regimes based on the ratio of h/L where L is defined as $L = (2\kappa/g^{1/2})^{2/3} = 2.53$ km. Considering this, three dynamic regimes are as follows: (1) $0 \leq h/L \leq 0.5$ where diffusion is adequately strong; (2) $0.5 \leq h/L \leq 2.0$ where diffusion and advection are in balance; and (3) $h/L \geq 2.0$ where advection dominates over diffusion.

The methods including procedures and steps used in the current study involved data inputs, estimation processes, and outputs. All numerical values for the geomagnetic field F_z were obtained for free from www.ngdc.noaa.gov/IAGA/vmod/ (International Association of Geomagnetism and Aeronomy [IAGA], 2016) in the form of geomagnetic coefficients issued for the 12th Generation of International Geomagnetic Reference Field (IGRF), numerical data for the global bathymetri of sea depth h were also obtained for free at www.ngdc.noaa.gov/mgg/global/relief/ETOPO1/ (National Geophysical Data Center [NGDC], 2016), numerical data for maximum amplitudes of the sea surface elevation η for four large tsunamis, namely: the 2010 Chilean, the 2011 Tohoku, the 2010 Mentawai, and the 2004 Aceh were also freely available at www.ngdc.noaa.gov (National Oceanic and Atmospheric Administration [NOAA], 2016). For comparison, careful visual inspection upon magnetogram freely accessible at www.intermagnet.org (INTERMAGNET, 2016) and www.bcmt.fr (BCMT, 2016) was then performed.

Analytical estimates of b_z and b_H have used equations (2) and (3) for tsunamis triggered by large earthquakes, that is, the 2010 Chilean and the 2011 Tohoku events as the two events satisfy criteria for *frozen-flux* approximation. For the 2010 Mentawai tsunami, a number of field data were consistent with advection case requirement ($c/c_s \approx 1$ and $h/L \geq 2.0$) where *frozen-flux* approximation remained effetive, and other data records were partially at a regime where oceanic diffusion effects started to influence (*intermediate regime*) and the rest were classified into the dominant diffusion regime. Therefore, estimate of b_z for the Mentawai tsunami used equation (4) but values of b_H for the same case were still estimated using equation (3). The 2004 Aceh tsunami is here discussed in comparison with that of the Mentawai. Outputs of all cases considered in this study are values of b_z and b_H obtained from analytical estimates for cases either with *frozen-flux* or with no *frozen-flux* approximation and visual estimates through inspection on either magnetogram provided by INTERMAGNET and BCMT or relevant graphs of magnetic variations recorded by magnetic instrument deployed at the sea floor, such as Ocean Bottom Electromagnetometer (OBEM).

RESULTS AND DISCUSSIONS

Two large tsunamis firstly discussed are the Chilean event that occurred on 27 February

2010 with the epicenter is located at 36.1° S and 72.6° W, tsunami origin time (OT) at 06:44 Universal Time Coordinates (UTC), and magnitude of M_W 8.8 and the other that occurred in Tohoku on 11 March 2011 with the epicenter at 38.3° N and 142.4° E, tsunami OT at 05:51 UTC, and magnitude of M_W 8.9. Table 1 contains complete data listing names of magnetic station with their corresponding geographical positions, numerical values of F_z, η and h obtained from relevant sites previously stated, and the vertical component b_z calculated using equation (2). IPM, PPT, and KAK are names of magnetic station while B14 (one of OBEM as used by Ichihara et al., 2013) is sensitive instrument deployed at the sea floor having the same function as magnetic station to monitor electromagnetic signals induced by tsunami waves.

Values for b_z in Table 1 are tested by recalculating them with respect to the effects of oceanic diffusion (see corresponding values in Table 2). Indeed, b_z is recalculated using equation (4) in which some physical quantities needed are as follows: $\kappa = (\mu\sigma)^{-1}$ with $\mu \approx \mu_o = 4\pi \times 10^{-7}$ WbA^{-1}m^{-1} (ocean magnetic permeability), $\sigma \approx 4$ Sm^{-1} (conductivity of seawater) and the complex speed of ocean waves c_s calculated from $c_s = (c^2 + c_d^2)^{1/2}$ where c and c_d are previously defined.

Table 2 provides recalculated values for b_z using equation (4), where the results differ by ≤ 7% from those calculated using equation (2). This discrepancy is considered insignificant hence frozen-flux approximation remains valid. This argument is supported by values listed in columns 4 and 8 in Table 2, where $h/L \geq 2.0$ and $c/c_s \approx 1$ are found in all monitoring stations for the two events. With respect to small perturbations of b_z from its maximum amplitude, frozen-flux theory is proved to be reliable and effective for use to estimate b_z accurately enough, in particular when diffucion effects are ignorable.

As previously written, estimates of b_z using both equations (2) and (4) are compared with records of magnetogram provided by the global network of INTERMAGNET and BCMT. Graphical magnetogram indicates that for the 2010 Chilean event there is a periodic signal of magnetic variations observed and measured by instrument at IPM seen in Figure 1 for magnetogram from INTERMAGNET and in Figure 2 for magnetogram from BCMT.

Figure 1 clearly shows effects of local disturbances on the sea surface due to earthquake with large magnitude that occurred off the coast of Chili, where the disturbances generated a giant tsunami wave propagating across the Pacific and then arriving at IPM 3500 km away from the epicenter. In turn, magnetic perturbations due to tsunami wave propagation were well recorded as the periodic signal b_z of the secondary field (denoted by three red-circles in the Z component of INTERMAGNET magnetogram). The periodic signal is obviously observed to occur around 11:45 UTC and provides a convincing clue for the magnetic anomaly with the mean value of the amplitude is best estimated at about 0.47 nT.

For comparison, Figure 2 provides magnetogram from BCMT for the same event. The periodic tsunami-magnetic signal was also re-

Table 1. Data for the 2010 Chilean and the 2011 Tohoku events with b_z is calculated using equation (2).

Tsunami Event	Magnetic Station	Latitude Position	Longitude Position	F_z (nT)	η (m)	h (m)	b_z (nT)
2010 Chilean	IPM	27.17° S	109.41° W	19019.6	0.15	6933	0.41
	PPT	17.57° S	149.57° W	18886.0	0.12	5085	0.45
2011 Tohoku	B14	39.03° N	144.48° E	37271.6	2.35	5830	15.02
	KAK	36.23° N	140.18° E	35619.2	4.50	10272	15.60

Table 2. Data for the 2010 Chilean and the 2011 Tohoku events with b_z is calculated using equation (4).

Tsunami Event	Magnetic Station	h (m)	h/L	c (ms^{-1})	c_d (ms^{-1})	c_s (ms^{-1})	c/c_s	b_z (nT)
2010 Chilean	IPM	6933	2.7	260.7	57.4	266.9	0.98	0.40
	PPT	5085	2.0	223.2	78.3	236.6	0.94	0.42
2011 Tohoku	B14	5830	2.3	239.0	68.3	248.6	0.96	14.45
	KAK	10272	4.1	317.3	38.8	319.6	0.99	15.49
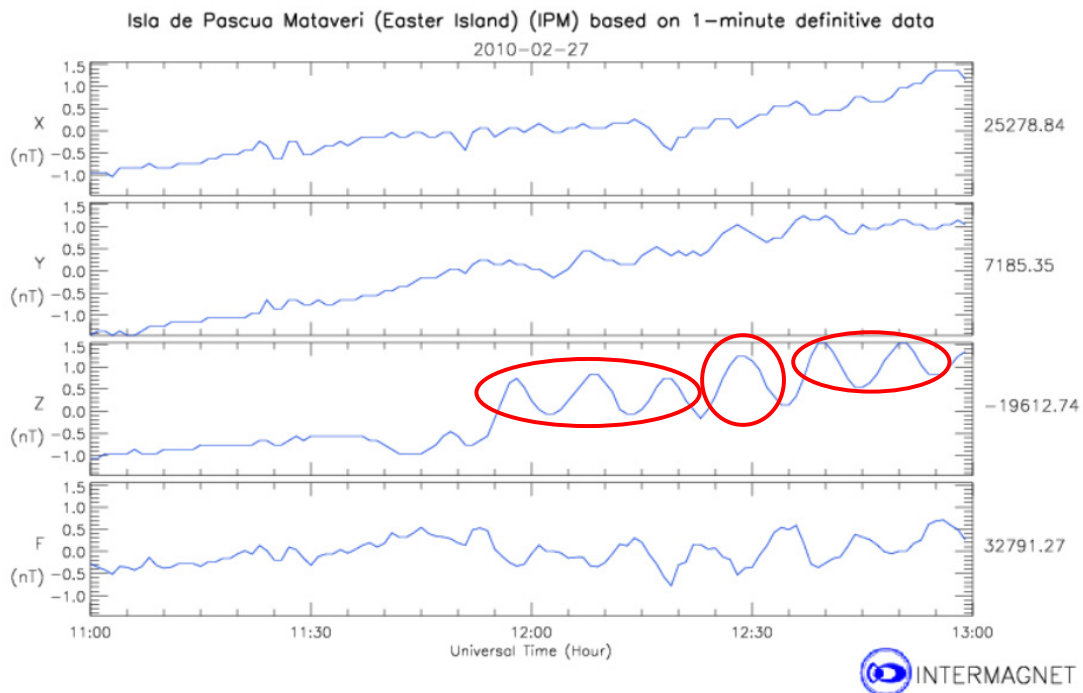
Figure 1. Magnetogram from INTERMAGNET for the 2010 Chilean tsunami occurrence recorded at IPM (3500 km away from the epicenter) after 5-hours travelling from the epicenter towards IPM.

corded at IPM run by BCMT, where the magnetic anomaly started to observe at 11:45 UTC with the mean amplitude of about 0.48 nT. This value is considered insignificant difference from that given by INTERMAGNET.

Data for magnetogram from both INTERMAGNET and BCMT are also in good agreement with variations in hydrostatic pressure at the ocean bottom measured by OBEM close to IPM location, where maximum hydrostatic pressure variation is estimated to be equal to $b_z \approx 0.50$ nT (Sugioka *et al.*, 2014). The amplitude of the signal is consistent with *peak-to-peak* variation of b_z at about 1.0 nT suggested by Manoj *et al.* (2011) for the same tsunami. A slight difference in the results between analytical estimates and visual inspection using magnetogram is attributed to inaccuracy of ocean depth measurements of *h* obtained from a world map of ocean topography from global bathymetri data.

Different from the 2010 Chilean case in which tsunami propagation was characterized by periodic signals, a giant tsunami triggered by the 2011 Tohoku tsunamigenic earthquake demonstrated a traveling *solitary wave*. This is seen in Figure 3 within time interval 6:45–7:45 UTC, where a significant increase in the variation of the vertical signal is estimated to be b_z ≈15.8 nT (red circle in Figure 3). This is in good

agreement with theoretical prediction for the magnetic anomaly of b_z based on *frozen-flux* approximation, which gives $b_z \approx 15.6$ nT (KAK in Table 1).

Analytical estimate dan visual inspection upon relevant magnetogram for the 2011 Tohoku event are consistent with field observations made by Ichihara *et al.* (2013) using magnetic instrument (OBEM) placed at the sea floor. They found that the vertical component b_z of the tsunami-magnetic signals varied in the range $b_z \approx$ 12-19 nT with the mean value of $b_z \approx$ 15.5 nT (see Figure 4).

In addition to good agreement with relevant previous work (Ichihara *et al.*, 2013; Zhang, Baba, Liang, Shimizu, & Utada, 2014), the research results in this study are also confirmed by the findings of Minami & Toh (2013), reporting impulsive signals of the vertical component variation b_z with the amplitude of about 3 nT. The signal was detected by electromagnetometer sinking at the sea floor in the North-West Pacific (NWP) *site* 1500 km away from the epicenter. The earthquake induced a devastating tsunami, hitting areas off the east coast of Tohoku on 11 March 2011.

Significant discrepancies in b_z between the value of b_z = 3 nT (Minami & Toh, 2013) and the ones of b_z = 15.6 nT (analytical estimate based on *frozen-flux* approximation with the
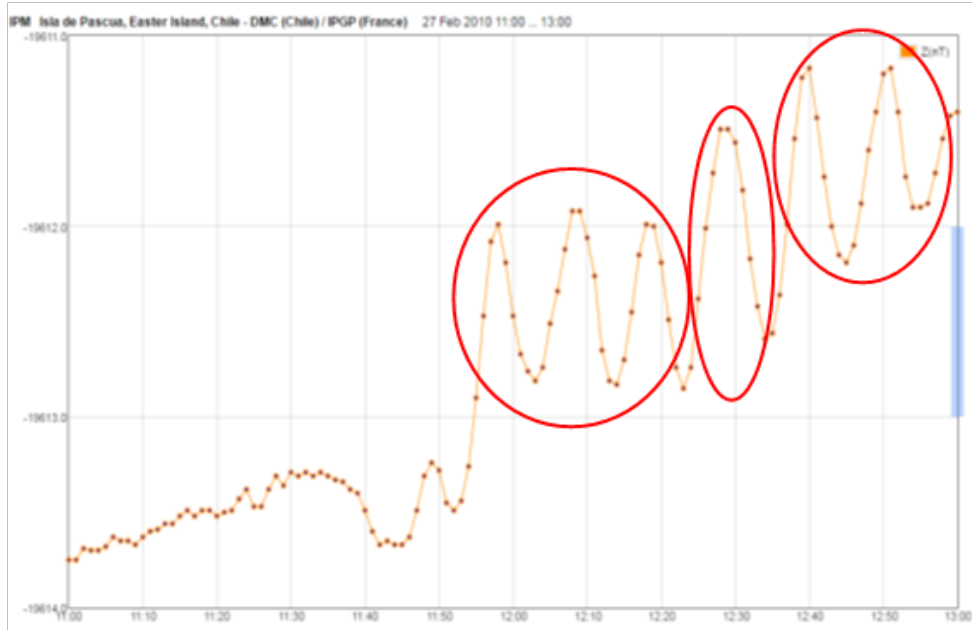
Figure 2. Magnetogram from BCMT for the 2010 Chilean tsunami occurrence recorded at IPM (3500 km away from the epicenter) after 5-hours travelling from the epicenter towards IPM.
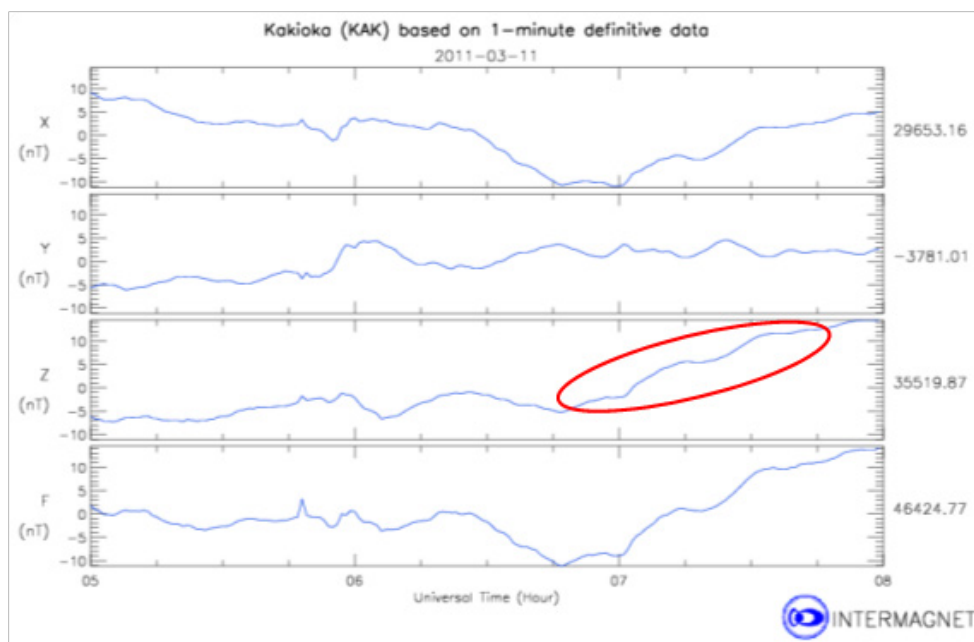
Figure 3. Magnetogram from INTERMAGNET for the 2011 Tohoku tsunami recorded at KAK (320 km away from the epicenter) within 1-hour travelling from the epicenter.

data from stasiun KAK) and b_z = 15.8 nT (visual estimate based on magnetogram from INTER-MAGNET) are due to the difference in observational locations. A simple calculation performed with respect to the geographical positions of magnetic instrument at the NWP *site* (Minami & Toh, 2013), B14 (Ichihara *et al*., 2013), and KAK as well yields the mean value of $b_z \approx 2.9$ nT for the 2011 Tohoku event, consistent with

the result of Minami & Toh (2013).

Figure 4 proves the maximum amplitude achieved for real time-varying of the vertical component b_z to be proportional to its corresponding sea surface elevation η monitored by a tsunami-gauge meter in the west Pacific (managed by NOAA) near the earthquake epicenter that generated Tohoku catastrophy. The proportionality between the two variables sup-

ports both theoretical estimates of b_z based on either *frozen-flux* approximation as predicted by equation (2) or calculation with the inclusion of diffusion effects as given by equation (4). The horizontal axis measured in minutes in Figure 4 below shows running time measured from earthquake OT. A high level of similarity is found in the variation of b_z between simulation on the basis of electromagnetic induction concept and *in situ* observations, particularly at tsunami *onset* time. This is clearly seen when the amplitude of the impulsive tsunami signal achieves its maximum value as shown by the red circle in Figure 4.
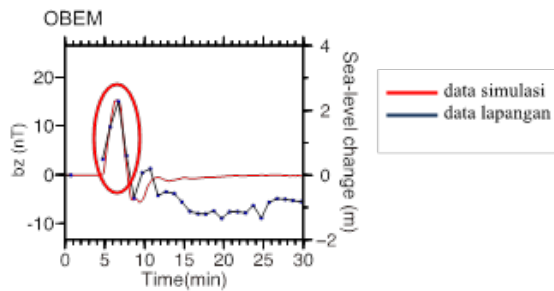
Figure 4. Time-varying of the vertical component b_z of the tsunami-magnetic field and its corresponding sea level change η from the 2011 Tohoku event recorded by B14, one of OBEM at the sea floor (250 km away from the epicenter), where $b_z \approx 15.5$ nT (taken from Figure 4, Ichihara *et al.*, 2013).

Theory of motional induction at seas describes not only the change in the vertical component b_z of the secondary magnetic signals relative to the primary geomagnetic field F_z but also the variations in the horizontal component b_H due to tsunami. In the context of time-varying of b_z two equations generally needed to estimate b_z are the one given by equation (2) used when horizontal advection is assumed to be the dominant process, widely known as *frozen-flux* approximation and the other given by equation (4) used when diffusion is somewhat important. In the context of time-varying of b_H the only formula for use in determining its maximum amplitude is given by equation (3) that holds for cases both with *frozen-flux* and with no *frozen-flux* approximation.

The followings are simple analyses related to equation (3). Firstly, replacing i with i = exp (iπ/2) and then writing the dependence of both b_z and b_H upon time t as

$$b_z = b_{oz} \exp (-i \omega t) \qquad (5)$$
$$b_H = b_{oH} \exp (-i \omega t) \qquad (6)$$

where b_{oz} and b_{oH} represent maximum amplitudes for the vertical b_z and horizontal b_H components, respectively. Secondly, substituting equations (5) and (6) as well as i = exp (iπ/2) into equation (3) yields

$$b_{oH} \text{ eks } (-i \, \omega t) = b_{oz} \text{ eks } \{-i \, (\omega t - \pi/2)\} \qquad (7)$$

Equation (7) clearly shows a phase difference in the tsunami-magnetic signals between b_z and b_H, where the horizontal signal b_H leads to the vertical signal b_z by π/2. As fluctuation of the secondary magnetic field is in the form of harmonic function of period T, the phase lag between the two signals is equal to the time interval $T/4$ required to achieve the maximum amplitude for each signal, with the horizontal component b_H achieves its maximum before the vertical component b_z does.

Within the context of the above mathematical analyses, T denotes the period of a tsunami wave that could be determined by simple uniform motion of the wave along its path. Some typical parameters needed to estimate T include the ocean depth of $h \sim 5000$ m = 5 km, the tsunami phase speed of $c = (gh)^{1/2} \sim 200$ m/s = 720 km/h, and the the tsunami wavelength of λ ~ 120 km. Taking these parameters all together, we have $T \sim 10$ minutes.

Figure 5 gives observational records for the horizontal b_H and vertical b_z of the secondary signals monitored by four magnetic instrument at the sea floor discussed in Zhang *et al.* (2014). All instrument named NM02, NM04, NM01, and NM05 and positioned at various locations with respect to the epicenter of the earthquake generating the 2011 Tohoku tsunami clearly indicate that the horizontal component b_H (represented by the dominant signal b_y in Figure 5) achieves its first peak before the vertical signal b_z. The b_y signals were respectively recorded at NM02, NM04, NM01, and NM05: 60 minutes, 64.44 minutes, 68.33 minutes, and 72.78 minutes whereas the b_z signals were observed at NM02, NM04, NM01, and NM05: 62.78 minutes, 66.67 minutes, 70.56 minutes, and 75.56 minutes, respectively, both records after *tsunami onset time* at 05:46 UTC. Based on the estimated arrival time difference between b_y and b_z signals at the accounted four stations (NM02, NM04, NM01, NM05), then the averaged arrival time difference for the two signals (b_y and b_z) to achieve their associated peak is about 2.5 minutes, in good agreement with $T/4$. This gains support from the work of Ichihara *et al.* (2013) stating that the dominant part of the horizontal component b_H is of b_y (b_y signal dominates over b_x signal as b_x signal is relatively weak) for the Tohoku event and that

the leading signal b_y precedes b_z by ~ 2 minutes.

The two large tsunamis, the 2010 Chilean and the 2011 Tohoku events, occurred at places of relatively deep waters with $h \geq 5100$ m such that $h/L \geq 2.0$ because of $L = 2.53$ km (Minami *et al*., 2015). The ratio of $h/L \geq 2.0$ is correlated with $c/c_s \approx 1$ (see Table 2). The data provided in Table 2 suggest that the deeper the ocean the larger the ratio of c/c_s. In other words, horizontal advection is stronger in places where the ocean is adequately deep and dominates over diffusion efects in the deep sea and therefore *frozen-flux* theory is effective for use to estimate b_z in such places. However, the effects of diffusion become unignorable in shallow waters where $h/L \leq 2.0$ (for example, the Indonesian waters). For cases where diffusion effects play a role in the dynamics of tsunami-magnetic signal generation, estimate of b_z is performed using equation (4) whereas estimate of b_H is still calculated using equation (3).

Table 3 below gives an example of the Mentawai tsunami that occurred on 25 October 2010 with the epicenter is located at 3.48° S and 100.14° E, tsunami OT at 15:00 UTC, and magnitude of M_W 7.8, where the depth of observational locations varies from relatively shallow to deep waters.

The data listed in Table 3 clearly show the ratio of $h/L < 2.0$ and $c/c_s < 0.9$ for the first four observational locations. The role of diffusion effects decreases much with increasing both h/L and c/c_s found in deep-sea places. For Cocos Island in the western Australian waters and Enggano in Bengkulu, the dominant process is advection and thus estimates of b_z in the two areas utilize the *frozen-flux* theory as predicted by equation (2) or the incorporation of oceanic diffusion effects into prediction as given by equation (4).

Observational location at Teluk Dalam in which the ratio of $h/L = 0.3$ and $c/c_s = 0.15$ indicates that a strong diffusion process is on duty. This is confirmed by a large deviation of b_z at a value of 84% from its true value based on calculation using equation (4).

Observational locations in Padang, Port Louis, and Rodrigues satisfy $0.5 \leq h/L \leq 2.0$ such that measurements of b_z are classified into *intermediate regime* (Minami *et al*., 2015). For Rodrigues, $h/L = 1.3$ and $c/c_s = 0.83$ the calculated value of b_z using equation (2) deviates from that when it is calculated using equation (4) by 17%. Such deviation reflects a dynamical balance between advection and diffusion.

The last two locations monitoring the Mentawai case in Table 3 demonstrate the

Table 3. Data for the 2010 Mentawai tsunami with b_z is calculated using equation (4).

Tsunami Event	Observational Location	h (m)	h/L	c (ms^{-1})	c_d (ms^{-1})	c_s (ms^{-1})	c/c_s	b_z (nT)
	Teluk Dalam	732	0.3	84.7	543.8	550.4	0.15	0.37
2010 Mentawai	Padang	1882	0.7	135.8	211.5	251.4	0.54	1.67
	Port Louis	2864	1.1	167.5	139.0	217.7	0.77	1.95
	Rodrigues	3261	1.3	178.8	122.1	216.5	0.83	2.15
	Cocos Island	6187	2.4	246.2	64.3	254.5	0.97	1.03
	Enggano	6699	2.6	256.2	59.4	263.0	0.97	0.71
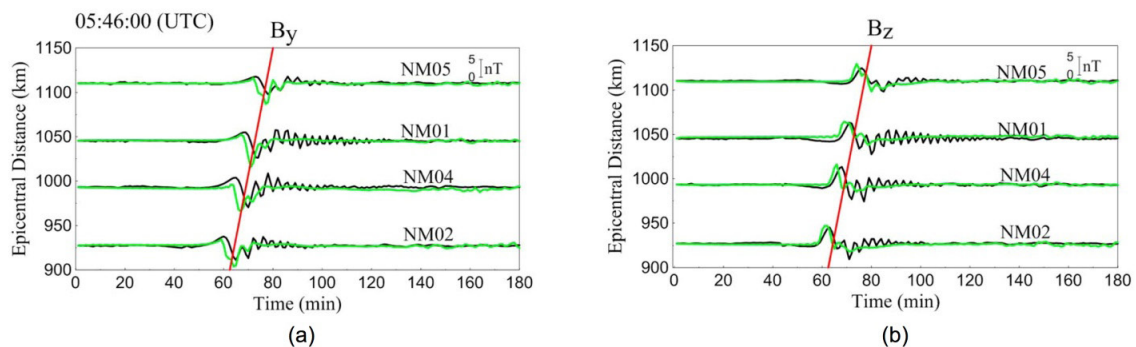
Figure 5. (a) The b_y signal representing the horizontal component b_H and (b) the vertical component b_z of the secondary magnetic field owing to tsunami for the 2011 Tohoku event recorded by four ocean bottom magnetometers named NM02, NM04, NM01, and NM05 (taken from Figure 1, Zhang *et al*., 2014).

dominance of horizontal advection over verti-cal diffusion as $h/L \geq 2.0$ and $c/c_s = 0.97$. This confirms that estimate of b_z in the two locations was performed using *frozen-flux* approxima-tion. The use of this approximation results in a small difference, of only 3%, in the calcula-tion of b_z between the calculated value given by equation (2) and the one given by (4).

The data for b_z listed in Table 3 also show a systematic increase in the magnetic distur-bance due to tsunami wave propagation, be-coming stronger as it approaches the zonal boundary between diffusion and intermediate regimes, reaching its maximum disturbed con-dition where b_z achieves it maximum value of 2.15 nT observed in Rodrigues, undergoing weakening effects when penetrating into ad-vection regime. This feature is well predicted by Minami *et al*. (2015).

The results for b_z estimates reported in Table 3 vary from 0.37 nT to 2.15 nT, consistent with both field measurements and numerical si-mulations of the vertical component of tsunami-magnetic signals obtained for areas near the equator. Tyler (2005) and Klausner *et al*. (2011) found a value of $b_z \leq 2,5$ nT for these areas.

However, the listed data in Table 3 for the 2010 Mentawai event confirm the maximum theoretical prediction for b_z based on *frozen-flux* theory that was proposed by Tyler (2005) after the most devastating tsunami hitting the west coast of Aceh in December 2004. The

catastrophy tsunami was difficult to handle be-cause there was no a well-developed, tsunami early warning system employed in the impac-ted areas, along the shorelines of Sumatranian west coast and surrounding the Indian Ocean. It was surprising that none of the local authority, such as BMKG nor global institutions, such as NGDC, NOAA and the Pacific Tsunami Warning Center (PTWC) managed instrument practically deployed for specific purposes on local deep sea research and regional sea surface monito-ring in the Indian Ocean. Therefore, empirical data for local perturbations at the sea surface elevation η and ocean depth h are not available in these areas and hence analytical estimates of magnetic anomaly using equations (2), (3), and (4) cannot be performed. Contrary to this, visual estimates through inspection upon mag-netogram for the case of Aceh tsunami remain available as given by both INTERMAGNET see in Figure 6 and BCMT seen in Figure 7.

Figure 6 describes local magnetic ano-maly caused by earthquake having the hypo-center below the sea surface at depth. The magnitude of the earthquake is of M_W 9.1 oc-curring on 26 December 2004 at 3.4° N and 95.7° E, and tsunami OT at 01:18 UTC. The red circle in Figure 6 shows *tsunami on-set* at 01:15 UTC.

Figure 7 provides magnetogram from BCMT for the same case as that in Figure 6, where PHU is located at 21.3° N and 105.95°
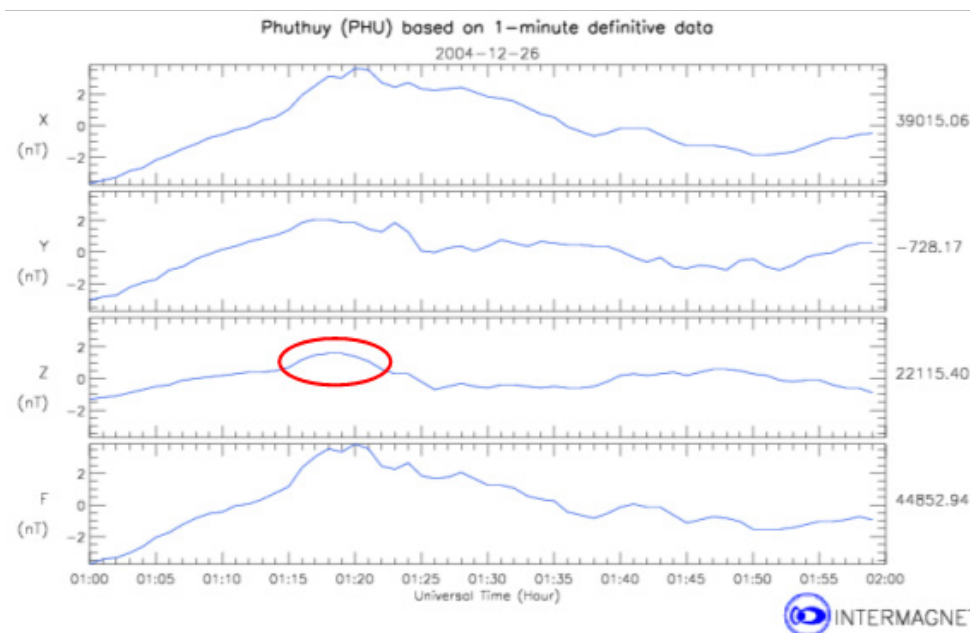
Figure 6. Magnetogram from INTERMAGNET for the 2004 Aceh occurrence recorded at PHU (Vietnam), showing $b_z \approx 1.8$ nT at the maximum amplitude of the tsunami-magnetic signal achieved.
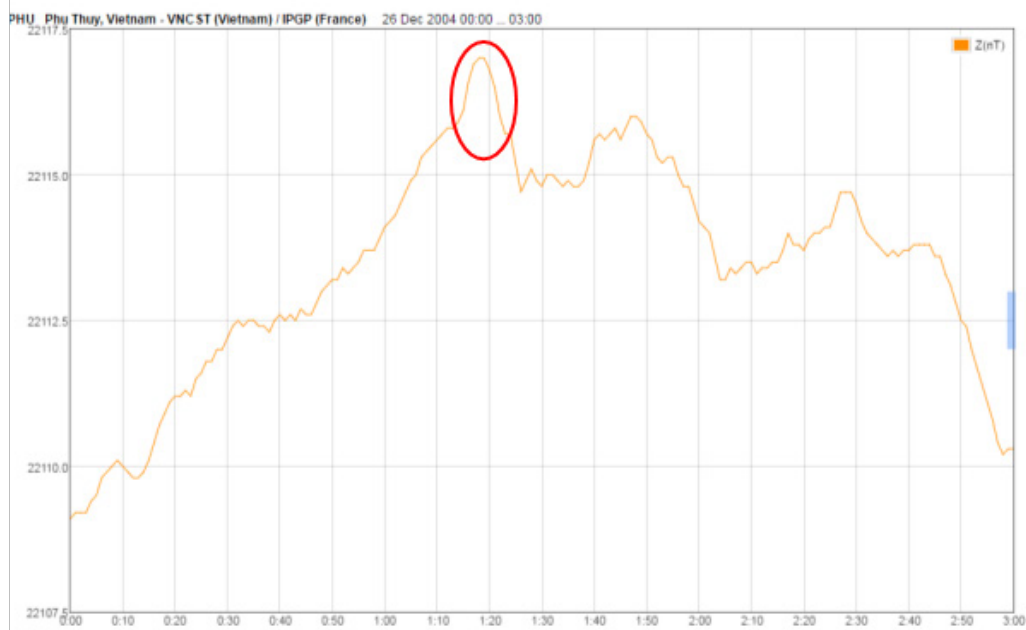
Figure 7. Magnetogram from BCMT for the 2004 Aceh occurrence recorded at PHU (Vietnam), showing $b_z \approx 2.0$ nT at the maximum amplitude of the tsunami-magnetic signal achieved.

E and confirms that the maximum amplitude of the vertical component b_z is found to be $b_z \approx 2.0$ nT (denoted by red circle), which was recorded within time interval 1:13–1:22 UTC, consistent with time interval observed for the same event provided by INTERMAGNET. The data records at PHU given by instrument managed by INTERMAGNET and BCMT are also in good agreement with magnetogram measured by similar instrument in AAE (Ethiopia) located at 9.02° N and 38.77° E, where $b_z \approx 2.5$ nT. The measured value of $b_z \sim 2$ nT obtained from the two stations is supported by the work of Klausner *et al*. (2011) using *wavelet* computational techniques.

Having analyzed the generation of secondary magnetic signals and local anomaly in the vertical b_z and horizontal b_H owing to tsunami passages for four large tsunami events, namely: the 2010 Chilean, the 2011 Tohoku, the 2010 Mentawai, and the 2004 Aceh with large, sea-hypocentered earthquakes and magnitudes of $M_W \geq 7.8$, some crucial points of views are discussed in the following paragraphs.

Firstly, the intensity of local anomaly signal is relatively small compared to the one produced by the Earth's fluid outer core, termed as the main geomagnetic field (Prastowo & Jannah, 2015). Therefore, the design and development of sensitive electromagnetic sensors for field monitoring and measurements of magnetic fields induced by ocean flow is a must. This is important because the success of real-time monitoring of any phenomenon in nature generally relies much on instrument accuracy and sensitivity. Hence, the advance of science and modern technology relevant to a particular earth-related disaster, such as tsunamigenic earthquakes and tsunamis, allows us to improve both the quality of measurement facilities for a better early warning system and the effectiveness of an approach to hazard mitigation study (Satriano *et al*., 2011; Satake, 2014).

Secondly, real-time monitoring of tsunami-magnetic signal and its corresponding local anomaly in the oceans examined in this study can therefore be an alternative method of the existing tsunami early warning system. This existing method has been based on seismic monitoring, for example, instrument for field measurements of seismic activities utilizing Global Positioning System (GPS) to rapid analyses of the earthquake size (Blewitt, Kreemer, Hammond, Plag, & Stein, 2006). Current studies relying upon seismic signal monitoring has included examination of subsurface seimo-tectonic activities covering areas in Sumatra (Santosa, 2012) and evaluation of accuracy in determination of some earthquake parameters for improvement of Ina-TEWS performance (Madlazim & Prastowo, 2016). Compared to these studies, the present method used in this study is promising and excellent in the sense that the developed method of tsunami-magnetic signal estimates, as predicted by equations (2) and (4), directly relates to a tsunami parameter,

that is, η, representing the maximum vertical sea surface displacement due to the passage of a tsunami wave at open seas. Knowledge of disturbance in the sea surface elevation η is required for better prediction of tsunami height (*water run-up*) when the giant wave approaches shorelines. Hence, this work is also important for hazard mitigation study.

Thirdly, in the context of hazard mitigation study a comprehensive approach is then necessary through careful handling on problems associated with 'front- (hulu) and end- (hilir)' user treatment and other relevant aspects as well. In the perspective of end-user treatment, information about the generation of tsunami-magnetic signals and magnetic anomaly could possibly be incorporated into school curricula through relevant educational and laboratory activities (Prastowo & Ain, 2015), and classroom activities on the basis of SETS and local wisdom (Rusilowati, Supriyadi, & Widiyatmoko, 2015). A combined approach of both types of treatment through integrated science in a classroom setting could also be implemented by providing students with discussions on mangrove plantation along a shoreline that is able to reduce ocean current and incoming wave energy hence to protect population living nearby (Kristiyanto, Armono, & Soemarno, 2013). In prinpicle, efforts in reducing disaster risks to minimum are thus compulsory for all authorities including educators, scientists, engineers, and decision makers to do the best for minimizing risks of disaster dan maximizing awareness of disaster-related science (Suppassri *et al.*, 2015).

CONCLUSIONS

Tsunami waves caused by large earthquakes with the hypocenter located below the sea surface generate secondary magnetic signals hence anomalies observed as small perturbations on the primary, Earth's magnetic fields. In this study, the secondary fields are then decomposed into the vertical b_z and horizontal b_H components and determined by analytical and visual estimates. Theoretical estimates of the two components depend on two interconnected parameters: h/L and c/c_s. If $h/L \geq 2.0$ and $c/c_s \approx 1$ hold (deep-sea cases with ignorable diffusion effects), then b_z is calculated using *frozen-flux* approximation. Using this approximation, estimate of b_z yields $b_z = 0.43$ nT for the 2010 Chilean event and $b_z = 15.31$ nT for the 2011 Tohoku occurrence. Values of

b_z found for the two large tsunamis are in good agreement with magnetogram from both INTERMAGNET and BCMT, where $b_z = 0.47$ nT for the 2010 Chilean case and $b_z = 15.80$ nT for the 2011 Tohoku tsunami. Another important result is that the horizontal signal b_H reaches at its maximum peak at about 2.5 minutes before the vertical signal b_z does.

The 2010 Mentawai event occurred in a relatively shallow water and is unique in that the roles of diffusion effects become into play. Some observational points show a large deviation of b_z estimates from the expected values, suggesting that prediction of b_z based on the *frozen-flux* theory is inapplicable to cases where oceanic diffusion is strong. However, the scatter of the calculated value for b_z in the range of $b_z \leq 2.5$ nT for this case is consistent with $b_z \sim 2$ nT recorded by magnetogram from INTERMAGNET and BCMT for the 2004 Aceh tsunami.

Monitoring of magnetic signals and anomalies due to tsunami can therefore be a candidate for tsunami early warning to assign a more comprehensive system in cooperation with the existing method based on seismic signal processing and monitoring. Good estimates of b_z and b_H, in agreement with prediction by visual inspection on magnetogram and the results from relevant previous work, however, have not yet unrevealed the characteristic of tsunami wave propagation. Issues, such as tsunami height when approaching the shoreline, tsunami propagation direction and its associated speed at open seas remain important and therefore such issues become challenging for future work.

ACKNOWLEDGEMENTS

REFERENCES

BCMT (2016). Data Plot. http://www.bcmt.fr/data_plot.php. Accessed on 20-21 April 2016.

Blewitt, G., Kreemer, C., Hammond, W.C., Plag, H., & Stein, S. (2006). Rapid determination of earthquake magnitude using GPS for tsunami

warning systems. *Geophysical Research Letters*, 33, 1-4.

IAGA (2016). Model field at a point by IGRF (IGRF-12). International Geomagnetic Reference Field/World Data Centre (IGRF/WDC) https://www.ngdc.noaa.gov/IAGA/vmod/igrf.html linked to http://wdc.kugi.kyoto-u.ac.jp/igrf/point/index.html. Accessed on 27 March 2016 and 18 April 2016.

Ichihara, H., Hamano, Y., Baba, K., & Kasaya, T. (2013). Tsunami source of the 2011 Tohoku earthquake detected by an ocean-bottom magnetometer. *Earth and Planetary Science Letters*, 382, 117-124.

INTERMAGNET (2016). Data-Plotting Service. http://www.intermagnet.org/data-donnee/dataplot-eng.php?type=xyz. Accessed on 20-21 April 2016.

Klausner, V., Domingues, M. O., Mendes, O., & Papa, A. R. R. (2011). Tsunami effects on the Z component of the geomagnetic field. August 25, 2011. physics.space-ph physics.ao-ph arXiv:1108.4893v1.

Klausner, V., Kherani, E. A., & Muella, M. T. A. H. (2016). Near- and far-field tsunamigenic effects on the Z component of the geomagnetic field during the Japanese event, 2011. *Journal of Geophysical Research*, 121, 1772-1779.

Kristiyanto, A., Armono, H. D., & Soemarno. (2013). Kemampuan hutan mangrove rumpun Rhizhophora SP dan Avicennia SP dalam meredam gelombang laut. *Jurnal Pendidikan Fisika Indonesia*, 9(2), 173-183.

Madlazim & Prastowo, T. (2016). Evaluation of earthquake parameters used in the Indonesian tsunami early warning system. *Earthquake Science*, 29(1), 27-33.

Manoj, C., Maus, S., & Chulliat, A. (2011). Observation of magnetic fields generated by tsunamis. *EOS*, 92(2), January 11, 2011, 13-14.

Minami, T., & Toh, H. (2013). Two-dimensional simulations of the tsunami dynamo effect using the finite element method. *Geophysical Research Letters*, 40, 4560-4564.

Minami, T., Toh, H., & Tyler, R. H. (2015). Properties of electromagnetic fields generated by tsunami first arrivals: classification based on the ocean depth. *Geophysical Research Letters*, 42, 2171-2178.

NGDC (2016). Bathymetric Data Viewer. National Centers For Environmental Information/ National Geophysical Data Center (NCEI/NGDC) https://maps.ngdc.noaa.gov/viewers/bathymetry/. Accessed on 27 March 2016 and 18 April 2016.

NOAA (2016). Recent and Historical Tsunami Events and Relevant Data. Pacific Marine Environmental Laboratory/National Oceanic and Atmospheric Administration (PMEL/NOAA) http://nctr.pmel.noaa.gov/database_devel.html. Accessed on 27 March 2016 and 18 April 2016.

Prastowo, T. & Ain, T. N. (2015). Percobaan *gravity current* untuk menguji konsep hidrodinamika dan hukum kekekalan massa pada fluida inkompresibel. *Jurnal Pendidikan Fisika Indonesia*, 11(1), 84-92.

Prastowo, T., & Jannah, A. (2015). Estimates of the earth's liquid outer core velocity using toroidal assumption and the DGRF/IGRF 1990-2000 magnetic models. *Proceedings of International Conference on Science and Science Education* (IConSSE), Faculty of Science and Mathematics (FSM), Satya Wacana Christian University (SWCU), August 1, 2015.

Rusilowati, A., Supriyadi, A., & Widiyatmoko. (2015). Pembelajaran kebencanaan alam bervisi SETS terintegrasi dalam mata pelajaran Fisika berbasis kearifan lokal. *Jurnal Pendidikan Fisika Indonesia*, 11(1), 42-48.

Santosa, B. J. (2012). Seismogram analysis of earthquakes in Sumatra-Java at HYB observatory station. *Jurnal Pendidikan Fisika Indonesia*, 8(2), 195-202.

Satake, K. (2014). Advances in earthquake and tsunami sciences and disaster risk reduction since the 2004 Indian ocean tsunami. *Geoscience Letters*, 1(15), 1-13.

Satriano, C., Wu, Y. M., Zollo, A., & Kanamori, H. (2011). Earthquake early warning: concepts, methods, and physical grounds. *Soil Dynamics and Earthquake Engineering*, doi:10.1016/j.soildyn.2010.07.007.

Sugioka, H., Hamano, Y., Baba, K., Kasaya, T., Tada, N., & Suetsugu, D. (2014). Tsunami: ocean dynamo generator. *Scientific Report on* www.nature.com. 4: 3596, 1-7.

Suppasri, A., Goto, K., Muhari, A., Ranasinghe, P., Riyaz, M., Affan, M., Mas, E., Yasuda, M., & Imamura, F. (2015). A decade after the 2004 Indian Ocean Tsunami: the progress in disaster preparedness and future challenges in Indonesia, Sri Lanka, Thailand and Maldives. *Pure and Applied Geophysics*, 172, 3313-3341.

Tatehata, H., Ichihara, H., & Hamano, Y. (2015). Tsunami-induced magnetic fields detected at Chichijima Island before the arrival of the 2011 Tohoku earthquake tsunami. *Earth, Planets and Space*, 67, 185-195.

Tyler, R. H. (2001). On the theory of magnetic fields generated by planetary oceans, *Proceedings of The Third Conference on Marine Electrodynamics* (MARELEC), Spearhead Exhib. Stockholm, Sweden.

Tyler, R. H. (2005). A simple formula for estimating the magnetic field generated by tsunami flow. *Geophysical Research Letters*, 32, L09608, 1-4.

Wang, B., & Liu, H. (2013). Space-time behaviour of magnetic anomalies induced by tsunami waves in open ocean. *Proceedings of The Royal Society* A. 469, 1-17.

Zhang, L., Baba, K., Liang, P., Shimizu, H., & Utada, H. (2014). The 2011 Tohoku tsunami observed by an array of ocean bottom electromagnetometers. *Geophysical Research Letters*, 41, 1-9.